AUSTROADS BRIDGE CONFERENCE 2025
Brisbane | 25-27 June 2025

Peer reviewed paper

SHS Signpost Fatigue Design: FEA & Experiment Validation

Mahdi Saadati, Senior Engineer, TfNSW

Hadi Alrawi, Lead Engineer, TfNSW

Saeed Saadati, Engineer, TfNSW

David Lowardi, Engineer, TfNSW

Abstract

The study presented in this report addresses the fatigue design of Square Hollow Section (SHS) signposts, which was identified as a gap by Austroads. Commissioned by Transport for New South Wales (TfNSW), the research aimed to develop a finite element model (FEM) for evaluating the fatigue performance of SHS sections, and to experimentally validate these models. The SHS sections investigated included 300x10, 200x9, and 125x9, all constructed from AS1163 350 grade material welded to AS3678 350 plate. The criteria for fatigue evaluation adhered to the AASHTO[1] Appendix C for the infinite life scenario. Experimental validation, conducted at the University of Queensland's Material Performance laboratory, involved testing the 125x9 SHS section to establish the maximum allowable bending moments for each SHS section. Results indicated the allowable bending moments as 5.20 kNm, 7.63 kNm, and 28.92 kNm for the 125x9, 200x9, and 300x10 sections, respectively. The experimental findings correlated well with the FEM predictions, with an acceptable average error margin of 7.8%, thereby confirming the model's reliability. These validated models are intended to inform the guidelines for the fatigue design of SHS signposts, ensuring their durability and safety in real-world applications.

Keywords: Fatigue, FEA, SHS, Validation, Bending

1. Introduction

AASHTO[1] 2015 (and earlier editions) provide guidelines for the design of structural supports for highway signs, specifying the use of round or multi-sided hollow sections for structural posts. However, SHS posts offer distinct design advantages such as easier fabrication due to flat surface and are widely utilised in Australia.

SHS support posts are typically butt-welded to base plates, which are subsequently bolted to footings. These welds are susceptible to fatigue cracking due to stress fluctuations induced by variable wind and traffic loads, as well as the inherent stress concentration at the square corners.

Austroads AP-G95-21[6], issued in 2021, identified a gap in the relevant standards regarding fatigue design assessment for SHS and RHS sections. Specifically, a direct relationship between applied bending moments and maximum stresses at the weld toe of SHS sections has not been established. In response, TfNSW aims to develop this relationship to inform fatigue design guidelines for SHS sections welded to base plates, following the methodology outlined in Appendix C of AASHTO[1] 2015.

2. Methodology

The objectives of this study were achieved through the following approach:

Finite Element Model Development:
A high-fidelity FEM was developed to determine the bending moment ranges that, in conjunction with the inherent stress concentrations of SHS sections, induce the criterion stress range defined in AASHTO[1] 2015 Appendix C, Section C.3.2.2 – *Fatigue Resistance*. The load case considered was a force applied perpendicular to a single flat face of the SHS. In addition to evaluating stresses at the weld toe region, strain measurements were incorporated into the model to facilitate experimental verification.

Full-Scale Static Testing for FEA Validation:
A full-scale static test was conducted for one selected SHS size and base plate configuration to validate the FEM results. The test followed a single-sided (half-amplitude) loading approach, wherein half of the bending moment range was applied to the test specimen. Consequently, half of the stress range predicted by the FEM was expected to be measured, eliminating the need for a reversing load mechanism in the test setup.

Experimental Strain Measurement and Model Refinement:
Strain gauges were installed at critical locations identified in the FEM analysis. The recorded strain data were compared against FEM predictions to verify model accuracy. Any observed discrepancies were addressed by refining the boundary conditions of the FEM to achieve closer alignment with experimental results.

3. SHS Post Construction

The study considered three SHS sections: 125 × 9, 200 × 9, and 300 × 10. All SHS posts are fabricated from AS 1163[3]-350 CL0 grade material and are welded to AS 3678[4]-350 grade base plates.

The post-to-base plate connection utilises a 490 MPa yield strength filler material, conforming to either EN49XX or W50X specifications[10]. This welded connection complies with AS 1554.1:2004[5], specifically Table E1, condition T-C 4b, as shown in Figure 1.

Figure 1: welded connections specification

B-C 4b T-C 4b C-C 4b	Single bevel butt weld, T and corner joints, welded one side with backing strip	t	All	All	All	All	All
		Position	See θ	F & H	See θ	F & H	See θ
		G	See θ	See θ	See θ	5	See θ
		F_r	0	0	0	0	0
		θ	20 for F: G = 11 (B-C 4b only) 30 for F: G = 9 mm 45 for all: G = 6 mm	30 for F: G = 10 45 for H: G = 6	30 for F: G = 10 45 for V, H & OH: G = 6	30 for F & H	30 for F: G = 10 45 for V, H & OH: G = 6

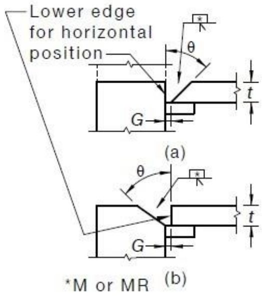

Reference : AS1554.1[5] Table E1 condition T-C 4b

125 × 9 SHS Test Specimen Preparation

The preparation of the **125 × 9 SHS** section for testing involved the following steps, as illustrated in **Figure 2**:

- **Backing Plate:** A **25 mm × 3 mm** backing plate was used, with **AS 3678[4]-250** grade material permitted.
- **Edge Preparation:** A **45-degree** edge preparation was applied to the SHS.
- **Weld Standoff Distance:** A **6 mm** standoff distance was maintained for the weld root.
- **Weld Type:** A **single bevel butt weld** was used to join the SHS to the base plate.

Figure 2: Weld detail for the 125 SHS test piece. Adapted from CW 9746 Rev E Sheet 3

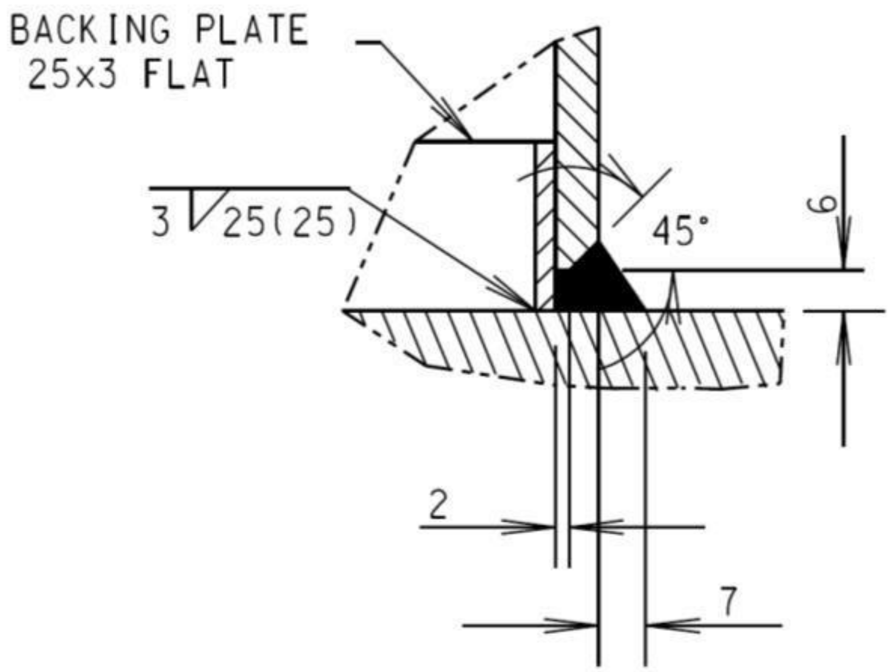

Bolted Connection and Snug-Tight Condition

The bolted connection on the base plate, as specified in the **design drawing supplied by TfNSW**, indicates a **snug-tightened** condition. According to **AS/NZS 5131[2]:2016, Clause 3.3.4**, snug tight is defined as:

"The tightness in the bolts in a bolted connection is attained by a few impacts of an impact wrench or by the full effort of a person using a standard podger spanner to bring the plies into firm contact."

The standard does not specify exact torque values for achieving snug tightness. Consequently, the resource shown in **Figure 3** was used to determine appropriate torque values for the snug-tight condition in the experiment. These values were based on an **achievable input force of 250 N** for the standard tool geometries listed.

From this torque value, a **pre-load of 27 kN** was calculated for the **M20 and M30** bolts used in the **FEA model**.

Figure 3: Snug tight torque values.

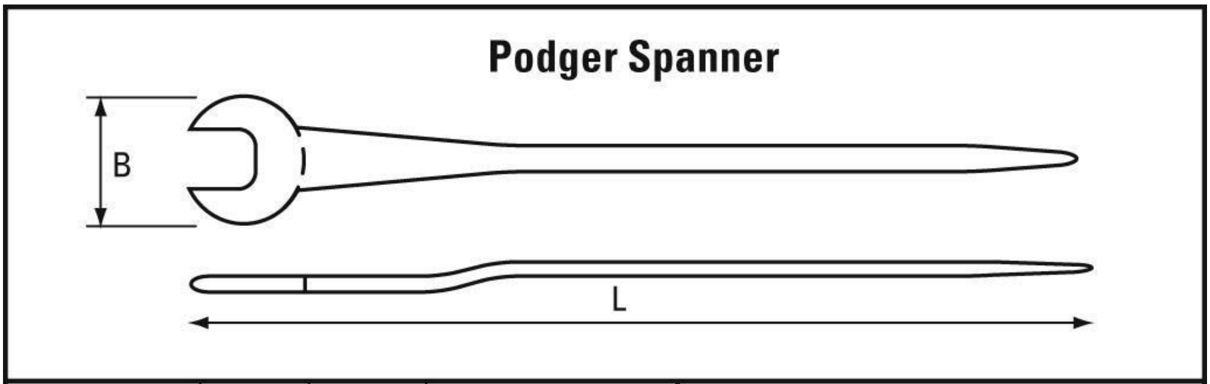

Bolt Size	B	L	Approximate Torque (Nm)
M16	60	460	90 *
M20	70	550	110 *
M24	85	640	130 *
M30	100	730	160 *

* Values are indicative of torque achieved when hand tightened using a force of 250N.

Reference: www.newsteelconstruction.com/wp/ad-302-tightening-of-ordinarybolts/

4. Finite Element Analysis

Setup

AASHTO **Appendix C** prescribes a methodology for assessing local stresses to ensure infinite life against fatigue cracking. This approach involves monitoring the **local stress at the weld toe region**.

In finite element analysis (FEA), a **zero-radius weld** would result in a theoretical **stress singularity** with an unbounded solution. To mitigate this, a **0.04 in (1 mm) radius** was introduced at the centre of the notch to provide a more realistic stress distribution.

The **FEA model meshing** included:

- **8 elements** along the notch perimeter to capture the stress gradient accurately.
- **Reduced integration 20-node solid isoparametric elements** to model the **connection and weld toe region**, ensuring numerical stability and accurate stress predictions.

Figure 4: Meshing in the weld toe regions for the AASHTO Appendix C criteria.

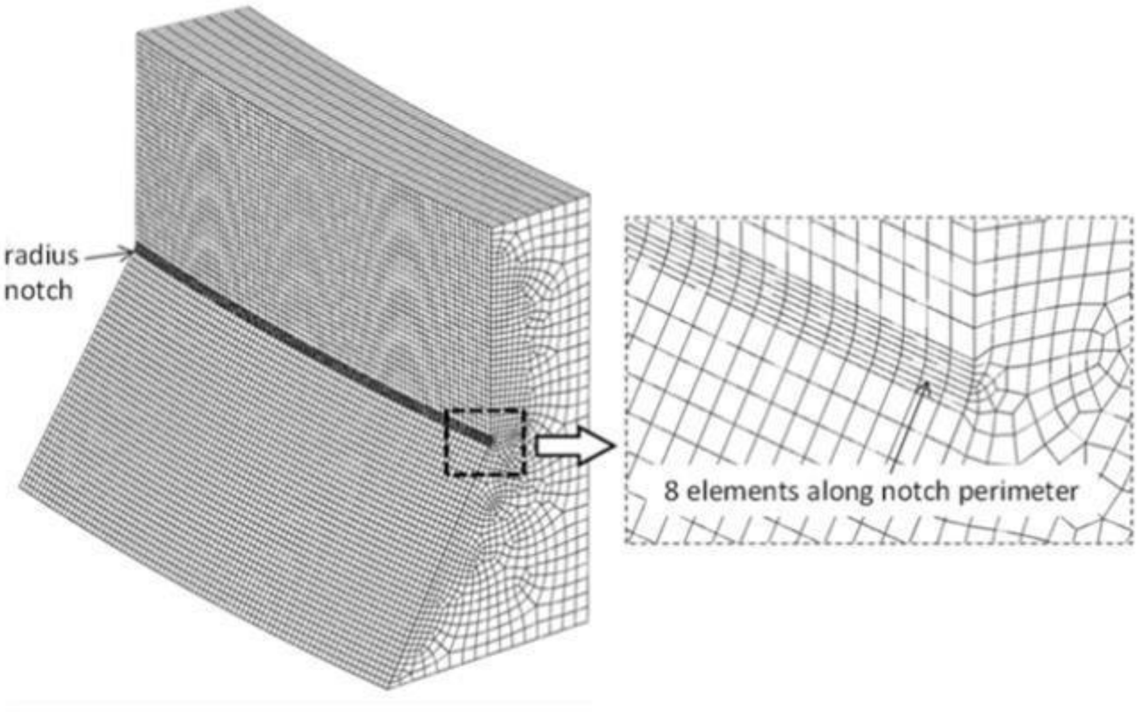

Allowable Local Stress Calculation

The allowable local stress in the notch is determined using **Equation C3.2.2-1** from **AASHTO Appendix C**, expressed as:

$$(\Delta F)_l = \frac{-F_y + \sqrt{{F_y}^2 + 4({F_u}^2)}}{3.2} \qquad 1$$

where

F_y = $material\ yield\ strength$

F_u = $material\ ultimate\ strength$

$$(\Delta F)_l = \frac{-350 + \sqrt{350^2 + 4(430^2)}}{3.2}$$

$(\Delta F)_l$ = 181 MPa

Table 1: Approximate Initial Forces for FEA Model

Section	Length of SHS (mm)	Force (N)	TfNSW Standard Drawing No
125x9 SHS	4700	860	CW9746E
200x9 SHS	5040	2343	ME10754J
300x10 SHS	6900	4512	ME16550A

FEA Setup and Mesh Generation

The finite element analysis (FEA) was conducted using **ANSYS 2021 R1**[8]. The mesh for the three SHS section sizes was generated using **ANSYS's built-in mesh algorithm**[8], ensuring adherence to the requirements outlined in **AASHTO**[1] **Appendix C**. The resulting meshes for each section size are shown in **Figure 5**, illustrating the mesh density and refinement at critical areas such as the weld toe and notch regions.

Figure 5 : (a) Meshing within the weld toe for 125x9 SHS, (b) Meshing within the weld toe for 200x9 SHS (c) Meshing within the weld toe for 300x10 SHS.

(a)	(b)	(c)

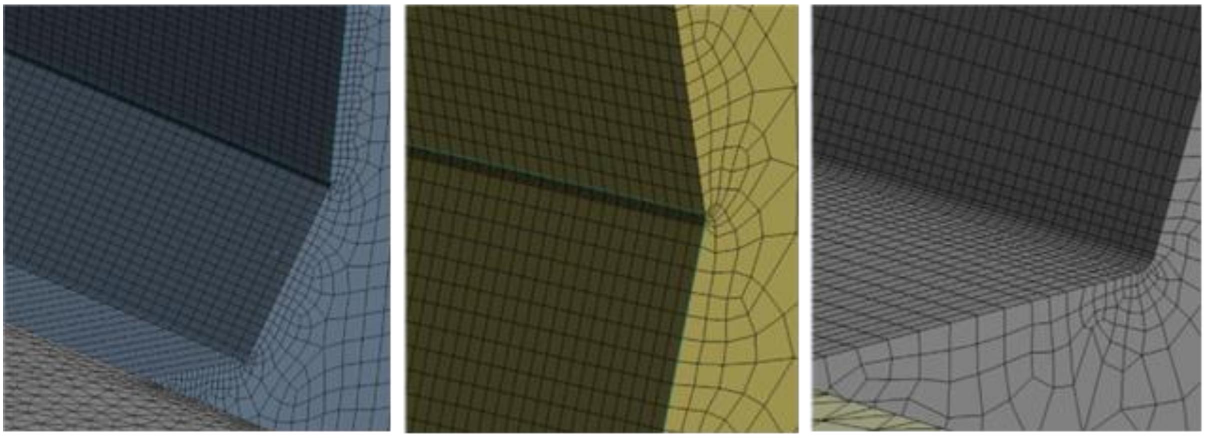

Load Cases

The finite element analysis (FEA) models were simulated both with and without **bolt tensioning** to assess the impact of pre-load on the stress distribution in the welded connection.

- **With Bolt Tensioning:** The bolt pre-load was applied based on the calculated **27 kN** pre-load from the snug-tight condition, considering the effect of bolt tension on the overall stress distribution and fatigue performance.
- **Without Bolt Tensioning:** This simulation excluded the bolt pre-load to evaluate the stress response solely from the applied external loading, without the influence of bolt-induced forces.

Figure 6: (a) Load case for 125x9 SHS without bolting pretension, (b) Load case for 200x9 SHS without bolting pretension, (c) Load Case for 300x10 SHS without bolting pretension.

(a)	(b)	(c)

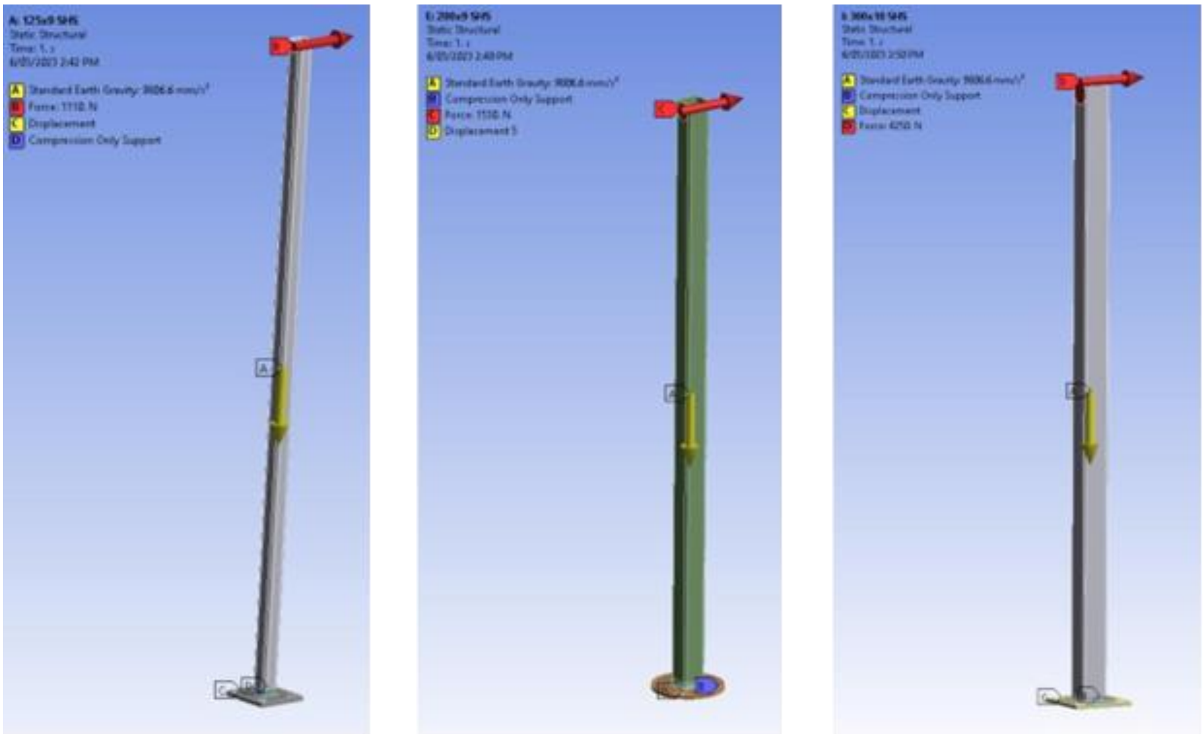

Boundary Conditions

The load cases for the SHS are shown in **Figure 6**. Each of the posts was modelled using the **longest SHS length** as specified in the drawings provided by **TfNSW**, with a **point load** applied at the tip of the post.

The **boundary conditions** for these models were as follows:

- **Vertical Support:** A vertical support was applied at the **washer clamping area** (illustrated in **Figure 7**) to restrict movement and simulate the base plate attachment.
- **Lateral Compression Support:** A **lateral compression-only support** was applied at the **bolt holes** (shown in **Figure 7**) to account for the interaction between the bolt and the post, ensuring proper modelling of the clamping forces.

Figure 7: (a) Displacement boundary condition for models without pretension, (b) Compression only support boundary condition for models without pretension.

(a)	(b)

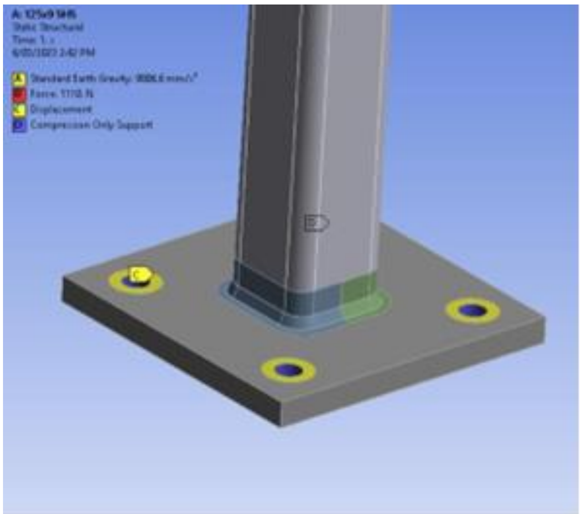

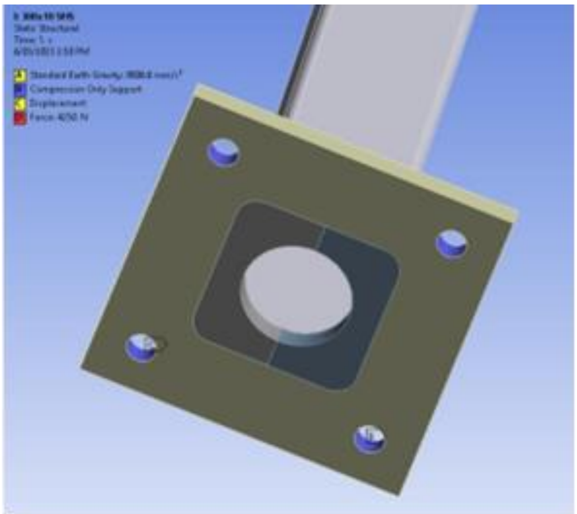

Bolting Pre-Tension Consideration

To evaluate the impact of mounting on the performance of the SHS section, an additional set of FEA simulations was performed in which the SHS was mounted onto a **'dummy' plate**. The dummy plate was fixed on its open surface, as depicted in **Figure 8**, and a **frictional contact** with a coefficient of **0.2** was applied between the **base plate of the SHS** and the dummy plate.

Fasteners were modelled, and a **pre-tension of 27 kN** (as shown in **Figure 8**) was applied to the bolts before the main loading event, simulating the snug-tight condition. The resulting load cases for each SHS section size, incorporating this pre-tension, are displayed in **Figure 9**. These simulations provide insight into how bolt pre-tension influences the overall stress distribution and fatigue performance of the SHS posts.

Figure 8: (a) Enlarged view showing the pre-tension top view (b) Bottom view

(a) (b)

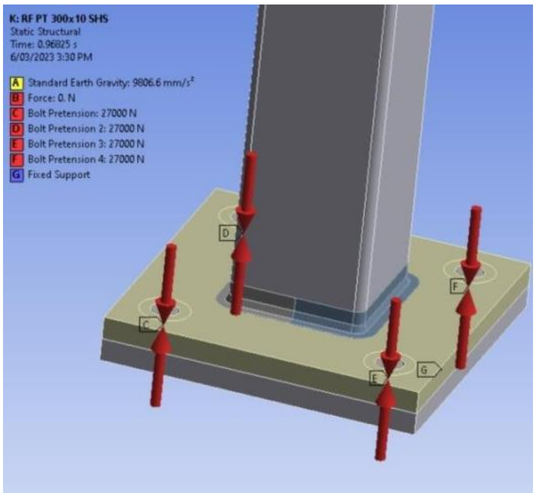

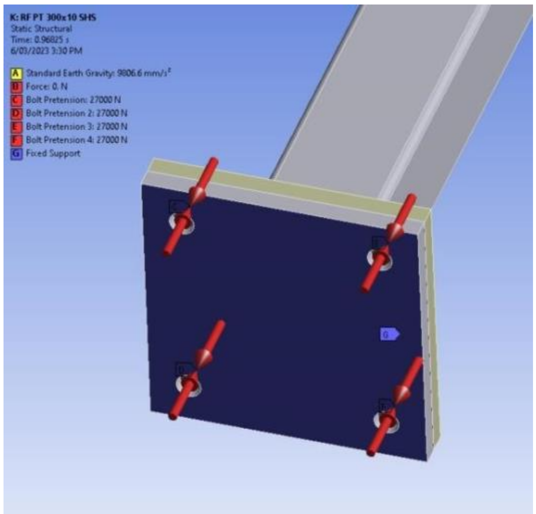

Figure 9: (a) Load case for 125x9 SHS, (b)Load case for 200x9, (c) Load case for 300x10 SHS. 27kN bolting pretension applied

(a)	(b)	(c)

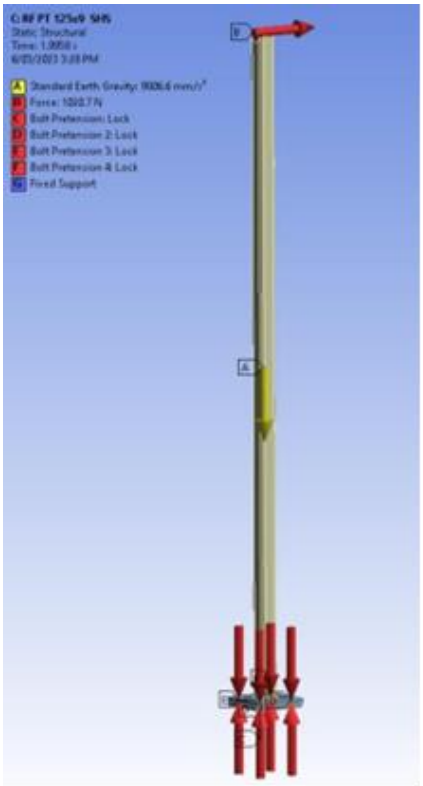
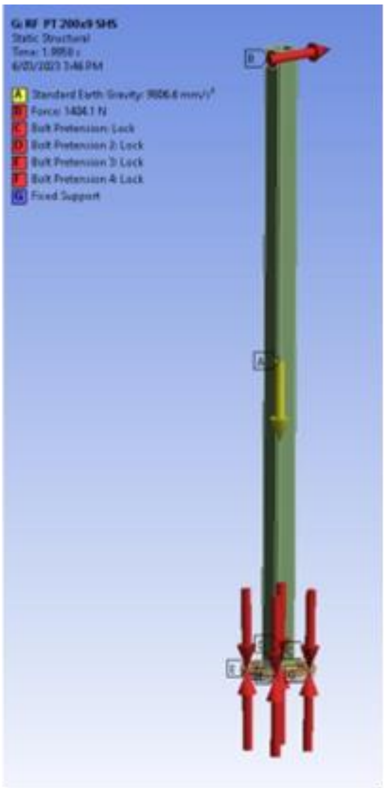


Results

The allowable forces and bending moments for both the standard and pre-tensioned FEA models are presented in **Table 2**. It was observed that the allowable force and bending moment for the **pre-tensioned model** were **lower** than those for the **standard model**.

Through an iterative process, the **peak forces** applied to the pre-tensioned model were adjusted to ensure that the stress within the **weld toe region** remained below the **181 MPa** limit, as per the fatigue resistance criteria. These iterations helped determine the maximum allowable forces and bending moments for the pre-tensioned condition, reflecting the impact of bolt pre-tensioning on the fatigue performance of the SHS sections.

Table 2 Allowable Applied Force and Bending Moments for SHS Section Sizes

	125x9 SHS	200x9 SHS	300x10 SHS
No Pretension Force	1110 N	1530 N	4250 N
No Pretension BM	5.20 kNm	7.63 kNm	28.92 kNm
With Pretension Force	1025 N	1410 N	2790 N
With Pretension BM	4.85 kNm	7.11 kNm	20.43 kNm
Difference	-6.7%	-6.8%	-29.4%

FEA Results Analysis

For the **125 × 9** and **200 × 9** sections, the allowable bending moment was reduced by **6.7%** and **6.8%**, respectively, when pre-tensioning was considered. However, for the **300 × 10** section, the effect of including pre-tensioning resulted in a **29.4% reduction** in the allowable moment.

The significant discrepancy observed for the 300 × 10 section is likely due to the **27 kN pre-tension load** being insufficient to generate the required moment to match the boundary conditions of the standard model. This was particularly evident in the results for the **300 × 10 SHS section**, where **compressive stress** was notably absent around the **washer contact area** for the fasteners, as shown in **Figure 10**.

In contrast, the **200 × 9 section**, shown in **Figure 10**, exhibited a more typical stress distribution. This suggests that **bolt torque during mounting** will play a critical role in ensuring the performance of the SHS post in real-world conditions, especially for larger sections where the applied pre-tension load may need to be higher to achieve desired performance levels.

Figure 10: (a) Compressive stress around the washer contact area in blue for the 200x9 section, (b) Compressive stress around the washer contact area not discernible for the 300x10 section.

(a)	(b)

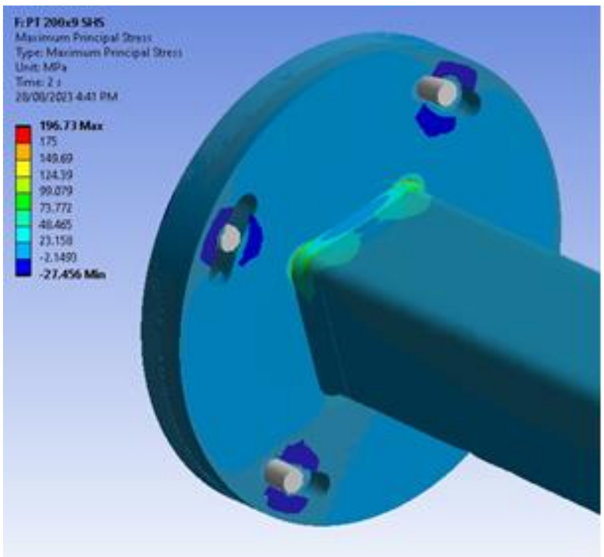

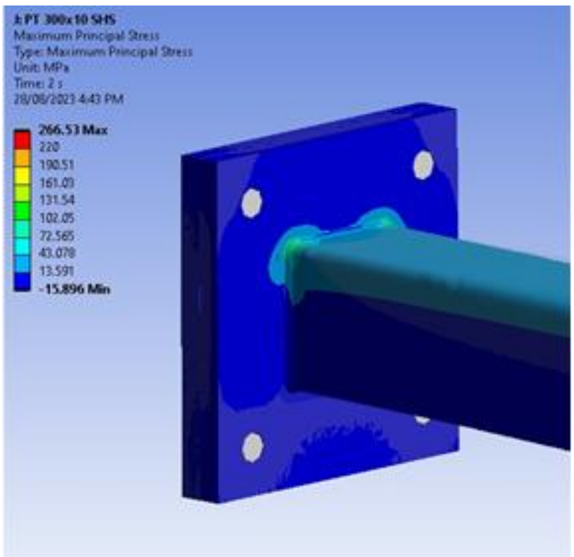

5. Mechanical Testing

Setup

Mechanical testing to verify the FEM was conducted at the **Civil Structures Laboratory** at the **University of Queensland Materials Performance Centre**. Due to mounting configuration constraints imposed by the testing facility, the **test piece** was mounted **horizontally**, as shown in **Figure 11**.

Figure 11: Experimental testing arrangement

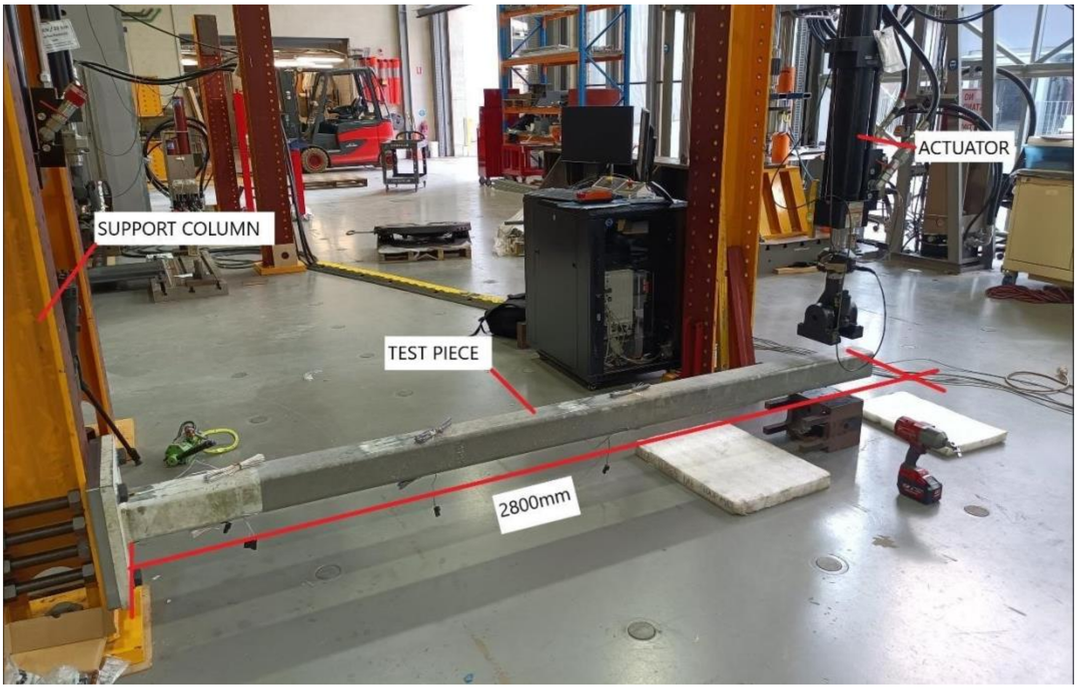

Mechanical Testing Procedure

Three **static tests** were performed by applying a **2000 N** load using a **100t actuator**, which was vertically directed onto the test piece at a distance of **2.8 m** from its base plate. To ensure even contact and consistent loading, the **head of the actuator** incorporated a **spherical bearing** design, as shown in **Figure 12**.

A total of **six strain gauges** were applied along the length of the SHS:

- **Two 120-ohm 45-degree rosettes** were placed at **15 mm** from the weld toe (Figure 12): one on the **top** to capture **tensile strain** and one on the **bottom** to measure **compressive strain**.
- **Two 350-ohm single-element gauges** were applied at **755 mm** from the base plate.
- **Two more 350-ohm single-element gauges** were placed at the **midpoint of the SHS**, **1510 mm** from the base plate (Figure 13).

These strain gauges provided critical data for validating the **FEA model** and verifying the stress and strain distributions predicted during the simulations.

Figure 12: (a) Head of the actuator contacting the test piece, (B) Supplied test piece SHS length measuring Notice the spherical bearing to ensure even load at 3020 mm for a total post length of 3052mm. application.

(a)	(b)

Figure 13: (a) Rosette strain gauges installed 15mm from the weld toe, (b) Location of single element strain gauges installed 755mm & 1510mm from the base plate of the SHS.

(a)	(b)

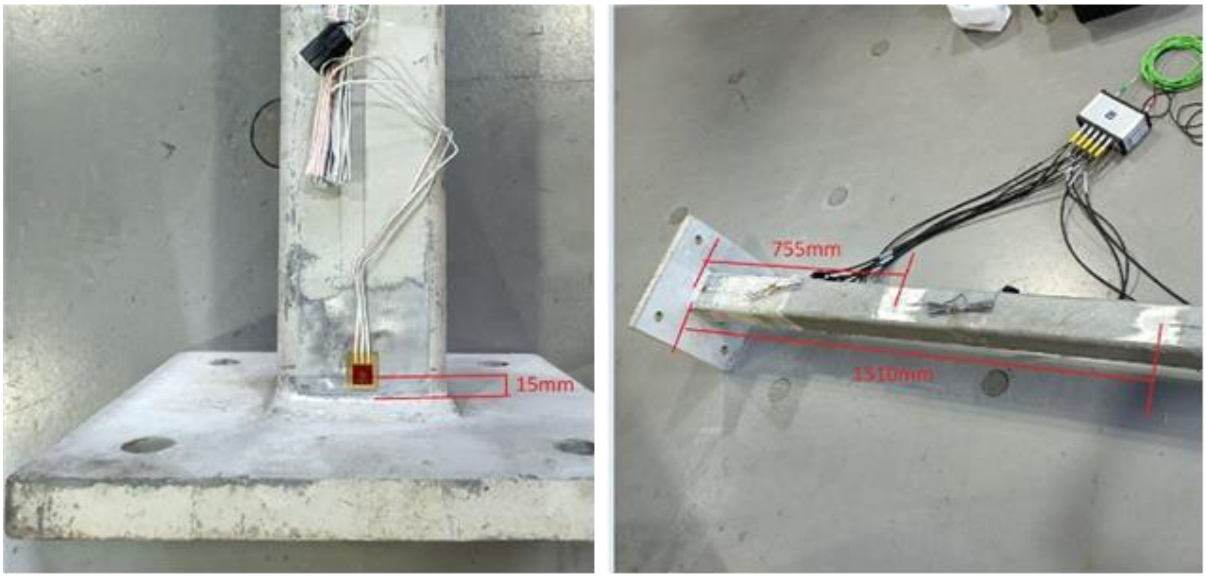

Data Acquisition System

The output from the **strain gauges**, totalling **10 channels**, was recorded using an **HBM[7]SomatXR MX1615B-R strain amplifier**, which was connected to a **laptop** running **HBM's Catman software** (version 5.4.2). This setup allowed for precise real-time data acquisition and analysis of the strain measurements during the mechanical testing.

For further details regarding the **testing setup** and configuration, additional information is available in the **report issued by the University of Queensland**[9].

Figure 14: The full experimental setup at UQ, showing the recording and measurement computers in the foreground and the test piece and actuators in the background

Figure 15: A screenshot showing the setup of the FEA model which replicated the UQ setup

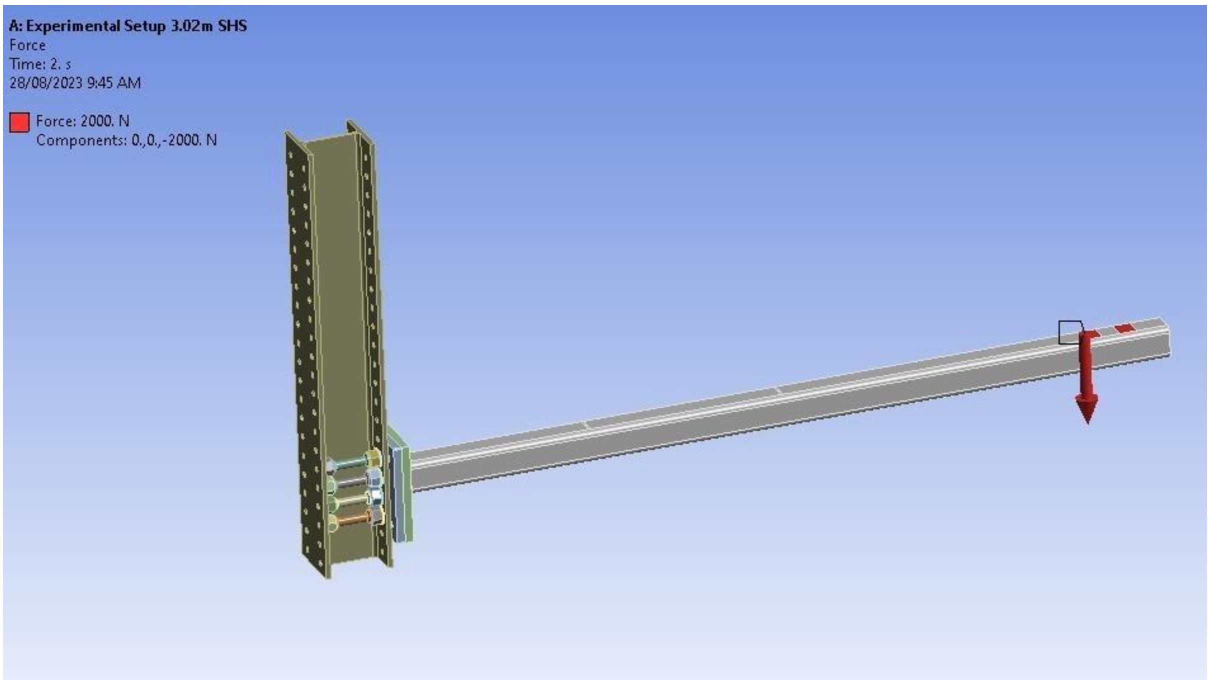

OFFICIAL

Comparison of Test Setup and FEA Model

Figures 14 & 15 present a **side-by-side comparison** of the **test setup** and the **FEA model**. After collecting the experimental data, adjustments were made to the **FEA model** to account for the previously mentioned **shorter post length**. Additionally, the model was further modified to closely align with the actual **experimental setup**, ensuring a more accurate representation of the real-world conditions during testing.

Results

The experimental results were compared to the finite element models using steel with varying **Young's modulus** values of **200 GPa**, **207 GPa**, and **215 GPa**. To replicate the zeroing effect that occurred during the experiment, the strain recorded in the FEA after applying pre-tension, gravity, and external load was adjusted by subtracting the strain recorded after the pre-tension and gravity load were applied.

Table 3 presents the comparison between the experimental data and the FEA using a **Young's modulus of 215 GPa**. Young's modulus provides the direct relationship between stress and strain in a material. By increasing the modulus from 200 GPa to 215 GPa, the correlation between the measured and predicted results improved, with an average error reduction of approximately **6.2%**.

However, an **outlier** was identified in the recorded measurements, specifically in the **top rosette** installed **15 mm** from the weld toe. The error percentage for this gauge was significantly higher than that of the other gauges. Additionally, the ratio between the **top** and **bottom strain** values at the two other measurement locations was **0.89** and **0.95**, but only **0.6** at this location. Despite the gauge providing repeatable results, these discrepancies suggest the possibility of either a **faulty gauge** or **poor contact** during installation. As a result, the strain values from this gauge were discarded for the validation process.

Table 3: Experimental Strain Results Compared to FEA (mm/mm) – Young's Modulus 215 GPa

Location	Measured (mm/mm)	FEA (mm/mm)	Difference (%)
15mm Top	1.25E-04	1.79E-04	+30.2%
15mm Bottom	-2.07E-04	-2.30E-04	+10%
755mm Top	1.23E-04	1.42E-04	+14.1%
755mm Bottom	-1.38E-04	-1.42E-04	+3.5%
1510mm Top	8.39E-05	8.95E-05	+7.7%
1510mm Bottom	-8.67E-05	-8.95E-05	+3.7%

Overall, the strain values recorded during testing were **lower** than those predicted by the FEA. The results showed a better correlation as the distance from the **weld toe** increased, particularly at the **1510 mm** location. For the five remaining gauges, the **average error** between the test and FEA was **7.8%**, which was considered acceptable for the testing process. This confirms that the testing successfully validated the FEA model.

After re-assessing the FEA in **section 4** with the higher **Young's modulus** of 215 GPa, no significant changes in the allowable bending moments for the three SHS sections were observed.

Additional Observations:

- The gauges on the **bottom** of the beam (under compression) exhibited **better correlation** with the FEA model compared to those on the **top**.
- The total **residual deformation** in the system after completing the three tests was **0.2 mm**.

- During the third test, the peak loading reached **2.155 kN**, but the strain and peak displacement associated with this peak load were excluded from the validation exercise.
- The **average displacement** recorded by the actuator during testing was **11.3 mm**, while the FEA model predicted **11.8 mm**, reflecting a **4.4% error**.

6. Discussion,

This article evaluates the suitability of the AASHTO Appendix C finite element analysis (FEA) method for performing fatigue checks on SHS (square hollow section) structures. To facilitate testing, modifications were made to the baseplate boundary conditions. In practice, baseplate support conditions can vary, ranging from full grout bedding to support on levelling nuts, or a combination of both, each providing different degrees of flexibility and typically resulting in lower stress concentrations. As such, the boundary condition adopted in the analysis represents a conservative assumption, ensuring that the results remain valid, and potentially more robust when applied to real-world scenarios.

7. Conclusion

The **finite element analysis (FEA)** results revealed the allowable bending moments for the **125x9**, **200x9**, and **300x10 SHS sections** as **5.20 kNm**, **7.63 kNm**, and **28.92 kNm**, respectively. These values align with the methodology outlined in **AASHTO 2015 Appendix C** for infinite life fatigue resistance. However, it is critical to emphasise that improper **tensioning** of the fasteners used to secure the posts can significantly affect their performance, and therefore must be carefully controlled.

Experimental validation of the FEA model was conducted at the **University of Queensland Centre for Material Performance**. The experimental results showed a strong correlation with the FEA, with an **average error of 7.8%**, which is considered within an acceptable range. This error margin suggests that the FEA model is slightly more conservative compared to actual conditions, providing additional confidence that the allowable bending moments derived from the FEA would be appropriate for real-world applications.

8. References

1. American Association of State Highway and Transportation Officials (2015) *AASHTO LRFD Bridge Design Specifications*, American Association of State Highway and Transportation Officials, Washington, D.C.
2. Standards Australia (2016) *AS/NZS 5131:2016 Structural Steelwork – Fabrication and Erection*, Standards Australia, Sydney, Australia.
3. Standards Australia (2009) *AS 1163-350: Structural Steel Hollow Sections*, Standards Australia, Sydney, Australia.
4. Standards Australia (2001) *AS 3678-350: Structural Steel – Hot-rolled Plates, Shapes and Bars*, Standards Australia, Sydney, Australia.
5. Standards Australia (2004) *AS 1554.1: Welding of Structural Steel*, Standards Australia, Sydney, Australia.
6. Austroads (2021) *AP G95-212: Guide to Fatigue Design of Steel Structures*, Austroads, Sydney, Australia.
7. HBM (2021) *SomatXR MX1615B-R Strain Amplifier Manual*, HBM, Germany.
8. ANSYS Inc. (2021) *ANSYS Mechanical 2021 R1 Documentation*, ANSYS Inc., Canonsburg, PA, USA.

9. University of Queensland (2025) *Experimental Results for SHS Post Fatigue Testing*, University of Queensland, Brisbane, Australia.

10. European Welding Standards (2021) *EN49XX, W50X Specifications: Welding Materials and Filler Specifications*, European Welding Standards, Brussels, Belgium.

Acknowledgments

We also acknowledge TfNSW for commissioning this study and providing essential input throughout the project. The authors would like to express their sincere gratitude to BMT Commercial Australia Pty Ltd for their support and collaboration.

Author contacts

Mahdi Saadati, TfNSW, Senior Engineer

Mahdi.Saadati@transport.nsw.gov.au, https://www.linkedin.com/in/m-saadati